PICOSECOND TRANSIENT THERMOREFLECTANCE:

TIME-RESOLVED STUDIES OF THIN FILM THERMAL TRANSPORT

Gary L. Eesley

Physics Department
General Motors Research Laboratories
Warren, MI 48090

The advent of new and sophisticated material growth processes (molecular beam epitaxy, chemical vapor deposition and ion sputter deposition) has produced new exotic materials such as amorphous alloys and compositionally modulated structures [1]. The atomic level structure of these materials can be proved by techniques such as x-ray diffraction. The electrical and thermal transport properties are also used to characterize these materials, which are usually deposited as thin films onto supporting substrates. Although the substrate may be electrically isolated from the film, complete thermal isolation is more difficult to achieve and thermal transport measurements are complicated.

A variety of optical, non-contact techniques have been developed to measure the thermal diffusivity of thin films. For instance, pulsed photo-thermal radiometry can be used to measure the thermal diffusivity of free standing metal films of known thickness [2]. This technique uses short laser pulses to heat the sample surface, followed by a time-resolved measurement of the black-body radiation to determine the surface cooling rate. Another method, photothermal deflectometry, has been used to determine thermal properties by measuring the optically-induced thermoelastic deformation of the surface or the heating induced refractive index gradient in a gas above the surface [3,4]. More recently, Rosencwaig et al. [5] have shown that a modulated thermoreflectance measurement is an equally sensitive method which can yield the same information as the deflection techniques. All of these techniques have been demonstrated with relatively low time resolution measurements, and in order to determine supported thin film thermal properties a knowledge of the substrate thermal properties is required. As a result, the accuracy of determining the film thermal diffusivity will depend on the precision to which the substrate thermal properties are known. The thermal impedance of the film-substrate interface can also complicate the determination of the film thermal properties. Although the theoretical treatments of heat flow in a simple multilayer system are correct, they only account for heat flow across ideal boundaries where there is an abrupt change in thermal properties [6-9]. In reality, many interfacial boundaries are characterized by strains, contamination and chemical interactions which can alter the thermal properties relative to the bulk values of the constituent materials. Detailed knowledge of the interfacial properties can be difficult to obtain and modelling of the heat flow may not be accurate.

As a solution to this problem, we have developed a technique which uses ultra-short laser pulses to generate transient thermoreflectance (TTR) signals which correlate with the transport of heat away from the film surface. Time-resolved measurement of these signals can be used to determine the thermal diffusivity of a supported film, independent of the substrate. In the following we will review the time domain analysis of thermal transport relevant to our technique. We will show how TTR can be used to study the thermal impedance of interfaces, in addition to measuring the thermal diffusivity of single element metal films. We will also show that on the picosecond timescale some interesting deviations from the standard heat flow equation can occur.

THERMAL TRANSPORT: TIME DOMAIN

In the classical theory of heat conduction, the heat flux J is directly proportional to the temperature gradient. For the case of one dimensional heat flow, this relationship can be expressed as

$$J(z,t) = -K\frac{\partial T(z,t)}{\partial z} \quad , \tag{1}$$

where K is the thermal conductivity and T is the temperature. When this flux is combined with the energy conservation equation

$$C\frac{\partial T(z,t)}{\partial t} = -\frac{\partial J(z,t)}{\partial z} + P(z,t) \quad , \tag{2}$$

we obtain the standard parabolic heat diffusion equation

$$C\frac{\partial T(z,t)}{\partial t} = K\frac{\partial^2 T(z,t)}{\partial z^2} + P(z,t) \quad , \tag{3}$$

where P(z,t) is a source term and C is the material heat capacity.

We are interested in the time response of the temperature increase produced by an incident laser pulse. In the case of metals, the optical radiation will be exponentially attenuated as a function of distance into the metal. If we assume a Gaussian shaped optical pulse of duration τ, and intensity I, the source term in Eq. (3) becomes

$$P(z,t) = I(1-R)\alpha R e^{-\alpha z} e^{-(t/\tau)^2} \quad , \tag{4}$$

where R and α are the metal reflectivity and absorbtivity, respectively. Substituting this heating source term into Eq. (3) and solving for the surface temperature as a function of time results in the curve shown in Fig. 1. This result represents the general response of a metal to an optical heating pulse with duration short compared to the time required for the heat to diffuse out of the heated volume. Here we have asssumed a 4 psec wide heating pulse, and the horizontal axis is labelled in delay time units; that is, time relative to the arrival of the heating pulse at the surface. Since the heating pulse has a finite duration, the zero time delay is defined to occur at the peak of the heating pulse intensity.

In thermal transport measurements, the decay time of the temperature is the quantity of interest. This decay time is directly related to the thermal diffusivity of the material, which is defined as

$$\kappa = K/C \quad . \tag{5}$$

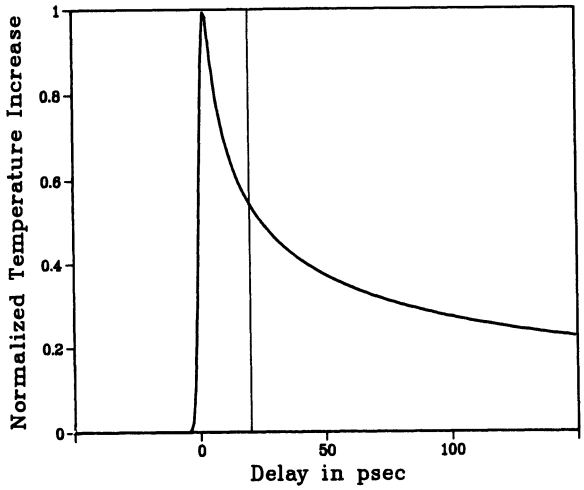

Figure 1. Calculation of the normalized temperature increase of the surface of a metal.

If the optical power is deposited at the surface of the medium, instead of in the heating depth $1/\alpha$, then κ would solely determine the decay time of the surface temperature. In reality, however, the finite heating depth must be accounted for in determining the temperature decay profile. As a result, the decay time depends on α as well. This is understandable since we are measuring the transport of heat away from the surface, and this occurs in a time on the order of $10/\kappa\alpha^2$. In Fig. 1, a thermal diffusivity of 2.3×10^{-5} m^2/sec and a heating depth of $1/\alpha$ = 14 nm were used.

Our discussion so far has only dealt with the macroscopic nature of thermal transport described by Eq. (3). Some interesting phenomena can be described if we consider the microscopic details of light absorption and thermal transport. In metals, the thermal conduction is dominated by the free electrons which absorb a fraction of the incoming optical pulse. The electrons which absorb the light thermalize very rapidly with the surrounding electrons and then cool by transferring energy to the metal lattice via electron-phonon scattering. This scattering process proceeds simultaneously with the diffusion of thermal energy down the temperature gradient. In Eq. (3), the thermal conductivity is that of the electrons, whereas the heat capacity used is that of the lattice. This is because the electronic thermal conductivity is much larger than that of the lattice. As a result of the electron-phonon coupling, the lattice heat capacity is used since it is much larger than that of the electrons. Thus the thermal diffusion is a coupled process, involving both the electrons and the lattice ion cores in a metal.

The validity of Eq. (3) in describing thermal transport really depends on the timescale we are considering. Clearly the electron-lattice temperature equilibration requires a finite amount of time. In metals this time is on the order of one picosecond (10^{-12} sec). Thus for heating pulsewidths of tens of picoseconds or longer, Eq. (3) describes both the electron and lattice temperatures. When the optical heating pulsewidth is comparable to or shorter than this equilibration time, then

we would expect a nonequilibrium temperature difference to exist between the electrons and the lattice. The fact that the electrons can be elevated to a temperature above the lattice results from the relatively small electron heat capacity.

Under these conditions the thermal transport and cooling process must be modeled by a two-temperature system of coupled differential equations, describing the electron temperature T_e and the lattice temperature T_i

$$AT_e \frac{\partial T_e}{\partial t}(z,t) = K\frac{\partial^2}{\partial z^2}T_e(z,t) - G(T_e-T_i) + P(z,t) \quad , \qquad (6)$$

and

$$C_i \frac{\partial T_i}{\partial t}(z,t) = G(T_e-T_i) \quad . \qquad (7)$$

In Eqs. (6) and (7), A is the electronic constant of heat capacity (linear in temperature, T_e), C_i is the lattice heat capacity and G is the electron-phonon coupling constant.

This nonequilibrium situation was postulated and modelled theoretically nearly thirty years ago [12]. Only recently have we been able to observe this phenomenon using picosecond pulsed lasers [13,14]. This nonequilibrium heating can be observed in both semiconductors and metals. With the advent of femtosecond (10^{-15} sec) pulsed lasers, time-resolved measurements of hot electron transport and electron-phonon relaxation are possible. On these ultrashort timescales, Eq. (6) predicts that hot electrons can be generated which transport heat with a thermal diffusivity much larger than that of the equilibrium transport in Eq. (3). That is, $K/AT_e >> K/C_i$, for temperature excursions of several tens of degrees.

A solution to the coupled equations (6) and (7) can also be found by the method of finite differences, and results for the metal copper are shown in Fig. 2. We have used a heating pulsewidth of 5 psec and a pulse energy of 0.5 nJ, and during this time we see that the electron temperature does exceed that lattice temperature by a few degrees [14]. The use of substantially shorter pulses results in a larger electron-lattice temperature mismatch, and the equilibration time exceeds the laser pulsewidth. Such studies are currently in progress using 80 fsec visible light pulses [15].

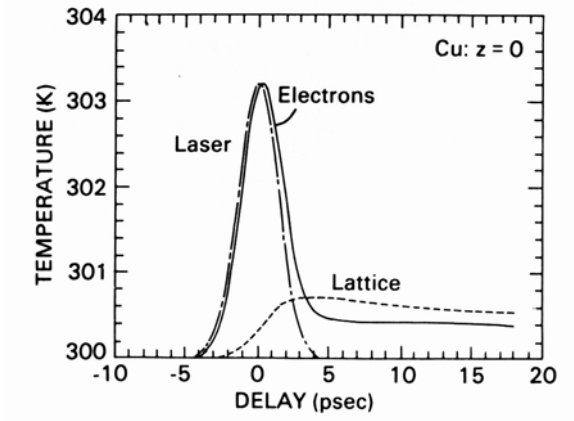

Figure 2. Calculation of the nonequilibrium heating of copper electrons. The laser heating pulse is centered at zero time delay.

The thermal transport processes we have discussed thus far have been based upon the heat flux of Eq. (1). When this flux is combined with the energy conservation equation, a heat diffusion equation is obtained. This equation predicts the instantaneous propagation of a thermal disturbance throughout the medium (see the Greens function in [10]). Despite this unrealistic result, these diffusion equations are quite accurate in modelling thermal transport in most situations. However, it has been shown that in situations involving transient heating at very low temperatures, the classical diffusion theory breaks down. Thermal transport takes the form of wave propagation with a finite velocity. This phenomena is referred to as second sound, in that phonon heat pulses have been observed to propagate macroscopic distances in a manner analogous to phonon acoustic pulses [16].

This deviation from the diffusion model can be accounted for by postulating a new heat flux equation

$$J + \tau_r \frac{\partial J}{\partial t} = -K\frac{\partial T}{\partial z} \quad . \tag{8}$$

When this equation is combined with the energy conservation equation (2), a hyperbolic differential equation is obtained

$$\frac{1}{v^2}\frac{\partial^2}{\partial t^2}T + \frac{1}{\kappa}\frac{\partial T}{\partial t} = \frac{\partial^2}{\partial z^2}T + \frac{P}{K} + \frac{\kappa}{v^2}\frac{\partial P}{\partial t} \quad . \tag{9}$$

In these equations, a propagation velocity v appears which is related to the thermal diffusivity κ by the relation

$$v^2 = \kappa/\tau_r \quad , \tag{10}$$

where τ_r is the thermal carrier relaxation time (electron-phonon relaxation time in conductors).

It is clear that in the limit of zero relaxation time, the propagation velocity becomes infinite and Eq. (9) reduces to the diffusion equation. Alternatively, if transient heating occurs on a timescale which far exceeds τ_r, then one would expect the diffusive nature of heat transport to apply. At very low temperatures(~1K) in solids, when τ_r is very large, the wave nature of thermal transport would become more apparent. Experiments have confirmed this phenomenon in solid helium and NaF crystals, where phonon mean free paths are comparable to the sample dimensions [17,18].

Beyond these rare situations, it is not clear that Eq. (9) is applicable or even necessary to describe thermal transport. Nevertheless there exists a core of literature on this subject, and solutions to the hyperbolic heat flow equation under a variety of conditions are well documented [19]. With the recent advances in generating ultrashort laser pulses for annealing and melting applications, it is possible that the wave nature of thermal propagation will be an important feature to consider in modelling heat transport at early times. In cases where film thicknesses are less than carrier mean free paths and heating pulsewidths are comparable to carrier scattering times, wave propagation at elevated temperatures may be observable. So far such observations have not been made, and the relevance of this form of transport is either overlooked or dismissed. It is a serious undertaking to generate realistic solutions to Eq. (9), and no attempt to do so will be given in this work.

TRANSIENT THERMOREFLECTANCE

Transient thermoreflectance (TTR) is a technique which uses two synchronous picosecond laser pulses to measure thermal diffusion. The first pulse produces ultra-fast heating to peak temperatures on the order of 10K above ambient. The second pulse has a variable delay with respect to the heating pulse, and it is used to measure the thermally-induced change in surface reflectivity($\sim 10^{-5}$/K). For small temperature deviations the reflectivity change is linear in temperature, and a temperature profile over several hundred picoseconds can be measured [11,20]. The penetration depth of visible light in a metal is approximately 20 nm, and thermal diffusion out of this region occurs in a few hundred picoseconds. Therefore, for film thicknesses of 100 nm or greater, the TTR measurement can be completed before substrate effects become important.

Since the heating depth is small compared to the diameter of the illuminated surface, a one-dimensional heat flow model can be fit to our measurements. Our fitting routine solves Eq. (3) by the method of finite differences. The routine involves a two parameter fit with the thermal diffusivity and a constant scaling factor as the free parameters. The accuracy of the fit is sensitive to the value of the optical absorption coefficient of the material, since we are monitoring the flow of heat out of the optical heating depth. We determine the complex refractive index of our samples by measuring the ratio of s-polarized to p-polarized reflectivity for both 30° and 70° angles of incidence. We fit these

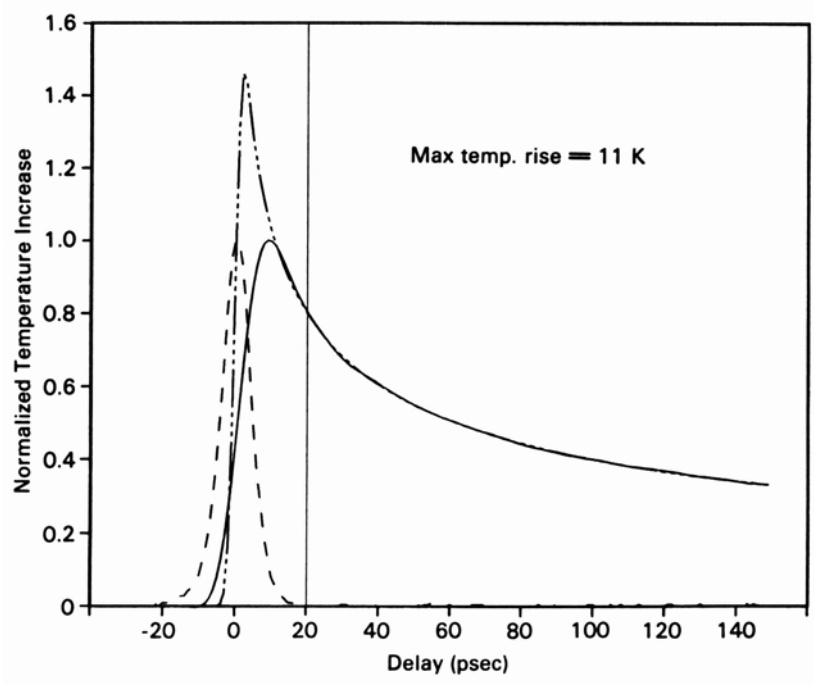

Figure 3. Best fit solution of the heat conduction equation to the normalized TTR measurement (solid line) of single crystal Ni. The cross correlation of the heating and probing pulses (long dash line) is also shown.

measurements to the Fresnel reflection formula and determine the real(n) and imaginary (k) parts of the metal refractive index. The imaginary part is then used to calculate the absorbtivity from the relation $\alpha = 4\pi k/\lambda$, where λ is the heating laser wavelength.

The validity of our approach for measuring the thermal diffusivity was initially tested by TTR measurements on bulk single-crystal nickel (110). Figure 3 shows the normalized TTR signal versus the time delay of the probing pulse relative to the heating pulse. Superimposed on the data is the best fit solution of Eq. (3) at z=0, calculated using a heating pulsewidth of 4 psec (full-width-at-half-maximum). The mismatch between the fitted solution and the data at early times is a result of convolution effects in the measured data which are not accounted for in the calculated temperature profile. These effects are only important at early times and we commence our fitting routine after a time delay of 20 psec. Thus the actual details of the heating pulse shape are not important [11]. The measured cross correlation of the heating- and probing-pulse is also shown in Fig. 3 to demonstrate the effective time resolution of our measurement and establish the zero time delay position. The thermal diffusivity fitted by our model is $\kappa = 2.1\text{x}10^{-5}$ m^2/sec, compared with the literature value of $2.23\text{x}10^{-5}$ m^2/sec [21]. The mean square error per data point is $5\text{x}10^{-4}$.

We have used TTR to measure the thermal diffusivity of deposited single element films and compositionally modulated Ni-Ti and Ni-Zr films [11]. We find that the thermal diffusivity of the modulated metal films is substantially smaller than that measured for the constituent single element films. This indicates that the interface between two different metallic layers can alter the thermal transport in a direction perpendicular to the film plane. Our goal is to use TTR to measure the thermal impedance of interfaces by fitting our results to a one-dimensional heat flow model which includes the interfacial boundary condition [9]

$$K_1 \frac{\partial T}{\partial z}1(1^-,t) = K_2 \frac{\partial T}{\partial t}2(1^+,t) = \frac{1}{\rho}[T_2(1^+,t)-T_1(1^-,t)] \quad . \quad (11)$$

K_1 and K_2 are the thermal conductivities of the metals on either side of the interface located at z=1. The thermal impedance of the interface is ρ.

We are currently implementing a fitting procedure which solves a heat flow equation appropriate to each single element region and coupled by the boundary condition in Eq. (11). We will use measurements of thermal diffusivity in single element films as input parameters to characterize the constituents in single interface, bilayer metal films. Our fitting routine will then determine the interfacial thermal impedance by fitting solutions of the coupled heat flow equations to the TTR measurement on the bilayer film.

Although the fitting procedure is not yet operational, we have performed a series of measurements of thermal transport across single metal-metal interfaces. The samples used for these measurements were fabricated to consist of a 30 nm Ni cap over a 300 nm metal underlayer of either Cu, Mo, Ti or Zr. The samples were prepared in a dual source magnetron sputter deposition system with a base pressure of 10^{-7} Torr. Silicon wafers were used as substrates under the simultaneously operating, shuttered sputter sources. Depostion rates were held constant at 0.5 nm/sec and the sputtering atmosphere was $2\text{x}10^{-3}$ Torr of argon.

A graphic example of the degradation in thermal transport produced by the presence of a single interface is shown in Fig. 4. TTR measurements are shown for both single element Ni and Ti films and for a Ni-Ti bilayer film. (All films are produced with the same sputtering conditions.) The decrease in thermal transport due to the metal-metal interface is clearly demonstrated and this effect is also observed in the other bilayer films [22].

Tabulated in Table 1 are the results of fitting our TTR measurements to a single heat flow equation (3) and determining an effective thermal diffusivity of the bilayer film. We have included measurements of the film optical properties as well. Figure 5 shows the TTR measurements for all four bilayer films investigated. The thermal diffusion is faster in the Ni-Cu film, followed by the Ni-Mo bilayer film. This ordering would be expected since the thermal diffusivities of Cu and Mo are larger than Ni, Ti and Zr.

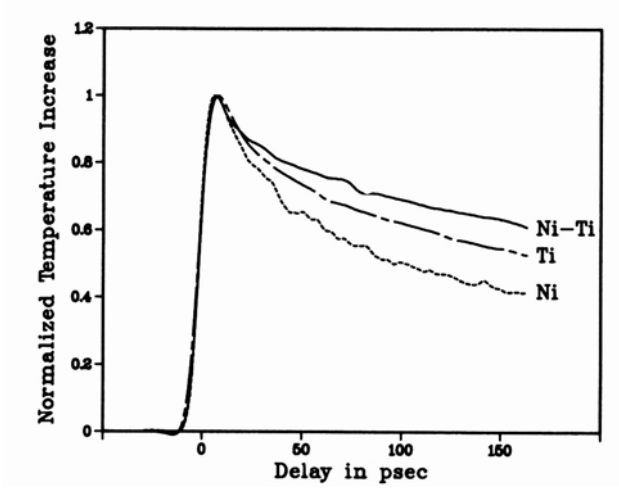

Figure 4. TTR measurements from single element Ni and Ti films, and from a single interface Ni-Ti bilayer film.

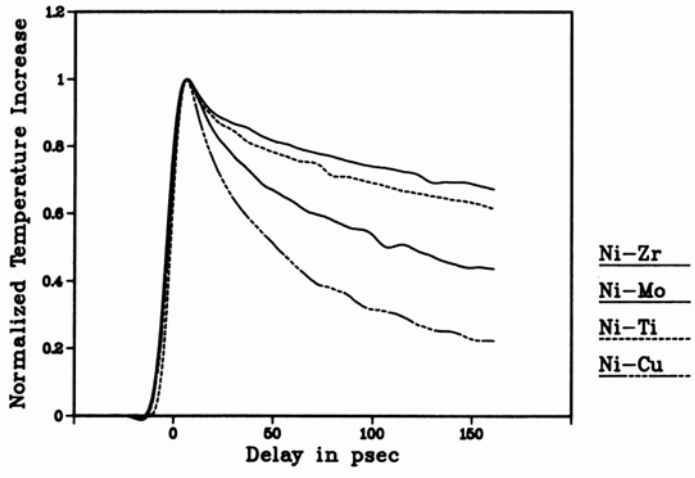

Figure 5. TTR measurements from different bilayer films.

A somewhat unexpected result is observed in the relative thermal diffusion of the Ni-Ti and Ni-Zr bilayer films. In this case we find that the diffusion in the Ni-Ti film is faster than in the Ni-Zr film, even though the thermal diffusivity of Zr is larger than that of Ti(see Table 1). We believe this reversal in trend may be attributed to the fact that the thermal impedance of the Ni-Zr interface is larger as a result of a larger atomic lattice mismatch and the ensuing higher degree of interfacial disorder. The relative lattice mismatch of the bilayer samples is calculated from literature values of nearest-neighbor lattice constants [23], and the results are also contained in Table 1. We find that the trend in degradation of thermal diffusion due to a metal-metal interface is correlated with the relative lattice mismatch of the metal constituents.

Table 1. The measured optical refractive index (n+ik), the absorptivity (α), the best fit thermal diffusivity (κ), and the lattice mismatch for both single element and bilayer films studied.

Sample		n	k	α ($\times 10^7$ m^{-1})	κ ($\times 10^{-6}$ m^2/sec)	Lattice Mismatch (%)
Ni	single element	1.80	3.71	7.4	4.4	-
Mo		3.07	3.84	7.6	12.5	-
Ti		2.34	3.28	6.5	1.5	-
Zr		2.13	3.31	6.6	2.5	-
Ni-Cu	bilayer film	1.73	3.70	7.3	32.0	2.8
Ni-Mo		1.80	3.85	7.6	6.1	9.2
Ni-Ti		1.63	3.54	7.0	0.42	16.1
Ni-Zr		1.81	3.80	7.5	0.33	27.3

The real atomic structure of our samples is currently being investigated by x-ray diffraction and the details will be presented in a later publication. We expect this analysis to provide more accurate mismatch values and a quantitative correlation with the interfacial impedance may be possible. What is clear at this point is that even between two metals, interfacial thermal impedance has a dramatic effect on thermal transport.

CONCLUSIONS

We have discussed the time domain analysis of the one-dimensional heat conduction equation, with the purpose of interpreting our picosecond time-resolved measurements of thermal diffusion in thin metal films. Our measurement technique is generally nonperturbative and provides a means of determining thin film thermal diffusivity independent of the supporting substrate. We have shown that the ability to do this is important because of the degradation in thermal transport produced by the presence of an interface. We expect that an additional advantage of ultrafast time-resolved measurements is the ability to measure interface thermal impedances in novel thin film structures.

We have shown that in the case of ultra-short heating, interesting nonequilibrium thermal transport can occur. This regime of thermal transport is important to fundamental studies of ballistic electron transport and electron-phonon relaxation in metals and semiconductors. The advent of laser heating sources in the femtosecond time regime may also require that we alter our conventional view of thermal transport as being diffusive in nature, at least over dimensions comparable to carrier mean free paths. Such dimensions are becoming more relevant as new growth techniques are being used to fabricate compositionally modulated materials with repeat distances on the atomic scale.

REFERENCES

1. Synthetic Modulated Structures, Edited by L. L. Chang and B. C. Giessen, Academic Press(New York, 1985).
2. W. P. Leung and A. C. Tam, Opt. Lett. 9,93(1984).
3. J. Opsal, A. Rosencwaig and D. L. Willenborg, Appl. Opt. 22, 3169 (1983).
4. L. J. Inglehart, K. R. Grice, L. D. Favro, P. K. Kuo and R. L. Thomas, Appl. Phys. Lett. 43, 446 (1983).
5. A. Rosencwaig, J. Opsal, W. L. Smith and D. L. Willenborg, Appl. Phys. Lett. 46, 1013 (1985).
6. M. Vaez Iravani and H. K. Wickramasinghe, J. Appl. Phys. 58, 122 (1985).
7. J. Baker-Jarvis and R. Inguva, J. Appl. Phys. 57, 1569 (1985).
8. J. Opsal and A. Rosencwaig, J. Appl. Phys. 53, 4240 (1982).
9. D. L. Balageas, J. C. Krapez and P. Cielo, J. Appl. Phys. 59, 348 (1986).
10. J. H. Bechtel, J. Appl. Phys. 46,1585 (1975).
11. C. A. Paddock and G. L. Eesley, J. Appl. Phys. 60, 285 (1986).
12. M. I. Kaganov, I. M. Lifshitz and L. V. Tanatarov, Sov. Phys. -JETP 4, 173 (1957).
13. G. L. Eesley, Phys. Rev. Lett. 51,2140(1983).
14. G. L. Eesley, Phys. Rev. B33,2144(1986).
15. R. W. Schoenlein, W. Z. Lin, J. G. Fujimoto and G. L. Eesley, in the conference proceedings of Topical Meeting on Ultra-fast Phenomena, Snowmass, CO (June 1986).
16. C. C. Ackerman and R. A. Guyer, Annals of Phys. 50, 128 (1968).
17. C. C. Ackerman and W. C. Overton Jr., Phys. Rev. Lett. 22, 764 (1969).
18. T. F. McNelly, S. J. Rogers, D. J. Channin, R. J. Rollefson, W. M. Goubau, G. E. Schmidt, J. A. Krumhansl and R. O. Pohl, Phys. Rev. Lett. 24,100(1970).
19. D. E. Glass, M. N. Ozisik, D. S. McRae and B. Vick, J. Appl. Phys. 59, 1861 (1986).
20. C. A. Paddock and G. L. Eesley, Opt. Lett. 11, 273 (1986).
21. American Institute of Physics Handbook,(McGraw-Hill, New York, 1972).
22. C. A. Paddock, G. L. Eesley and B. M. Clemens,presented at the International Quantum Electronics Conference, San Francisco, CA (June 1986).
23. C. Kittel, Introduction to Solid State Physics, 4th Edition, Ch. 1, Table 5(John Wiley and Sons, Inc., New York (1971).